Morphological Effects on Infrared Spectra

~ Experimental Spectroscopic Measurements of Free-Flying Particles~

A. Tamanai[1], H. Mutschke[1], J. Blum[2]

1. Astrophysical Institute and University Observatory, Friedrich-Schiller-University Jena, Schillergaesschen 3, D-07745 Jena, Germany
2. Institut für Geophysik und Extraterrestrische Physik, Technische Universität Braunschweig, Mendelssohnstra. 3, D-38106 Braunschweig, Germany

Correspondence to: akemi@astro.uni-jena.de

seit 1558

Introduction

Morphological effects (size, shape, and agglomeration) on the infrared (IR) spectra have been explored mostly via theoretical calculations (e.g. Mie 1908; Purcell & Pennypacker 1973; Bohren & Huffman 1983; Draine 1988; Mishchenko 1990; Mackowski et al. 1996; Min et al. 2005). However, these theoretical approaches do not satisfy all actual astrophysical dust grain conditions since the dust grains are various in size, complex in shape, intricate in agglomerate state, and composed of more than one species.

Although the KBr pellet technique has been widely used for spectroscopic analysis, the morphological condition of particles embedded in a KBr medium is hardly examined. By applying an aerosol technology, it is possible not only to obtain the IR spectra without a medium effect, but also to study the particle morphology by capturing the aerosol particles on a filter (Tamanai et al. 2006a & b).

We present the degree of morphological effects on the IR band profiles experimentally together with the particle images taken by a scanning electron microscope (SEM) and a transmission electron microscope (TEM).

Experimental Set-up

- A Fourier Transformation Infrared Spectrometer (FTIR, Bruker 113v) is attached to a White-type long-path infrared cell (MARS-8L/20V, Gemini Scientific Instr.) of 18 m path length and a detector box for measuring the extinction of the suspended dust particles in the cell (Fig. 1).
- Multiple reflection of the IR radiation between two gold mirrors at both ends of the cell enhances the sensitivity of the detection sufficiently to achieve optical depths around unity in the mid-IR bands.
- The dust flow generator (Palas RBG 1000), which utilizes a rotating brush to disperse a pressed powder from a dust storage hole into a nitrogen gas stream, produces the dense aerosol that is led through stainless steel tubes toward the cell.

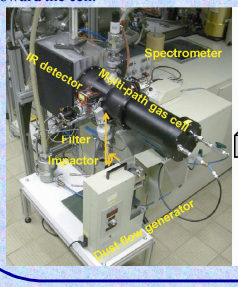

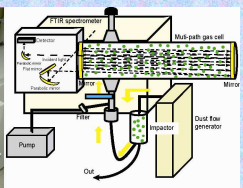

Fig. 1 Extinction measurement set-up (A photo & a schematic diagram)

Samples

43 samples of 10 compositions have been investigated so far.

	Chemical formula	Mineralogical name	Crystal structure	Particle size (μm)	Particle shape
1	SiO_2	Silicon dioxide	Amorphous	0.5	sphere
2	SiO_2	Silicon dioxide	Amorphous	1.0	sphere
3	SiO_2	Silicon dioxide	Amorphous	1.5	sphere
4	SiO_2	Silicon dioxide	Amorphous	5.0	sphere
5	SiO_2	Silicon dioxide	Amorphous	10nm-50nm	ellipsoids
6	SiO_2	Crestobalite	Crystalline	<1	irregular
7	Mg_2SiO_4	Forsterite	Crystalline	< 1	irregular
8	Mg_2SiO_4	Forsterite	Crystalline	~0.2	ellipsoids
9	$MgSiO_3$	--------	Amorphous	< 1	irregular
10	$Mg_{0.8}SiO_3$	--------	Amorphous	< 1	irregular
11	$MgSiO_3$	Enstatite	Crystalline	< 1	irregular
12	$MgSiO_3$	--------	Amorphous	< 1	irregular
13	$(Mg_{1.6}Fe_{0.4})SiO_4$	Olivine	Crystalline	< 1	irregular
14	Al_2O_3	Corundum	Crystalline (α-)	~0.3~0.5	irregular
15	Al_2O_3	Corundum	Crystalline (α-)	< 1	irregular
16	Al_2O_3		Crystalline (γ-)	~0.1~0.3	irregular (fluffy)
17	Al_2O_3		Crystalline (γ-/α-)	< 1	irregular
18	$MgAl_2O_4$	Spinel	Crystalline	< 1	irregular
19	$MgAl_2O_4$	Spinel	Crystalline	60nm	roundish
20	TiO_2	Rutile(Aldrich)	Crystalline (α-)	< 1	irregular with roundish edges
21	TiO_2	Rutile(Alpha)	Crystalline (α-)	< 1	irregular
22	TiO_2	Rutile(Tayca100W)	Crystalline (α-)	10-80nm	thin & long
23	TiO_2	Rutile(Chitan 101)	Crystalline (α-)	30-100nm	roundish
24	TiO_2	Anatase(A,long)	Crystalline (β-)	0.1-0.6	roundish
25	TiO_2	Anatase(U, cr)	Crystalline (β-)	0.1-0.2	roundish
26	TiO_2	Anatase(Tayca600)	Crystalline (β-)	10-50nm	roundish
27	TiO_2	Anatase(Chitan No.9)	Crystalline (β-)	~50nm	roundish & long-narrow
28	TiO_2	--------(A))	Crystalline	< 1	irregular
29	TiO_2	--------(Aldrich)	Crystalline	< 2	irregular
30	Ti_2O_3	--------	Crystalline	< 1	irregular
31	TiO_2	--------	Crystalline	< 1	irregular
32	$CaTiO_3$	Tielite	Crystalline	< 1	irregular
33	$CaTiO_3$	Perovskite	Crystalline	< 2	irregular
34	Mg-Fe-SiO_4	Mg-Fe-silicate	Amorphous	< 2	irregular
35	$Ca_{0.4}Mg_{0.6}Si_2O_6$	Diopside	Crystalline (natural)	< 2	irregular
36	$Ca_{0.4}Mg_{0.6}Si_2O_6$	Diopside	Crystalline (synthetic)	< 2	irregular
37	$(Mg_{0.9}Fe_{0.1})_2Si_2O_6$	Hypersthene	Crystalline (natural)	< 5	irregular&Stick
38	$(Mg_{0.9}Fe_{0.1})_2Si_2O_6$	Hypersthene	Crystalline (synthetic)	< 5	irregular
39	$CaSiO_3$	Wollastonite	Crystalline (synthetic)	< 2	irregular
40	$(Mg_{1.6}Fe_{0.4})Si_2O_4$	Olivine	Crystalline (natural:Afo.)	< 4	irregular
41	$Fe_{0.9}Si_2O_6$	Fayalite	Crystalline (natural)	< 5	irregular
42	$Al_2Si_2O_5(OH)_4$	Kaolinite	Crystalline (synthetic)	< 3	irregular&tabular
43	$Mg_3Fe_{0.1}Si_4O_{10}(OH)_2$	Talc	Crystalline (natural:Sparks)	< 2	irregular&tabular

Table 1: Properties of samples

1. Aerosol vs. pellet measurements (Medium effect)

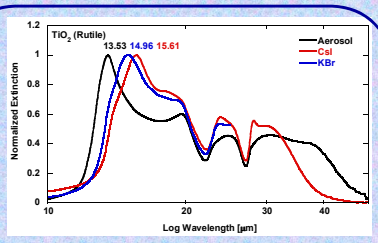

The peak shift depends on the dielectric functions of a sample (ε) and the embedding medium (ε_m) (Bohren & Huffman 1983). As the value of ε_m increases (N_2 1.0; KBr; 2.3; CsI 3.0), the peak positions significantly shift to the longer wavelengths by the influence of its electromagnetic polarization (Tamanai et al. submitted).

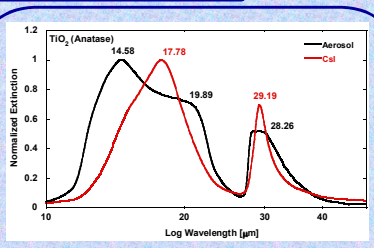

Band profile differences?

- Using different dispersion methods
- Particles may transform during the grinding procedure
- The powdered sample structure deformation due to the high pressurization required for the CsI pellet technique.

(Tamanai et al. submitted)

4. Morphological Effect (Agglomeration)

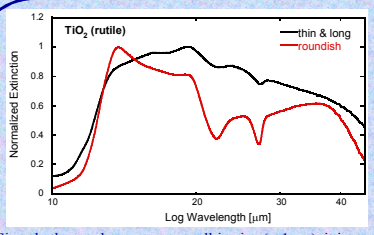

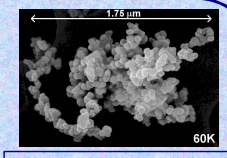

Sphere & ellipsoid d=0.01-0.1μm

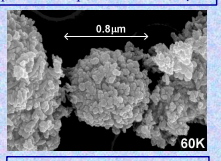

Thin & long d=0.01-0.08μm

Since both samples are very small in size (< 1μm), it is easy to form agglomerates. The roundish TiO_2 particles form fluffy agglomerates whereas close-packed agglomerates are composed of the thin & long shaped particles. The difference of the extinction band profile in the region 13-19μm in wavelength may be influenced especially by the agglomerate state (Tamanai et al. submitted).

2. Morphological Effect (Size)

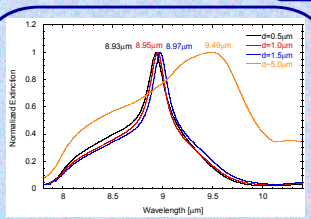

The spectra obtained by spherical amorphous silica (SiO_2) particles with diameter of 0.5, 1.0, 1.5 and 5μm are compared. As the particle size increases, the peak position shifts to longer wavelengths. Although small size particles constitute more agglomerates compared with the 5μm size particles, a peak position of the 5μm particles exceptionally shift to the longer wavelength and draw the band broadening (Tamanai et al. 2006a).

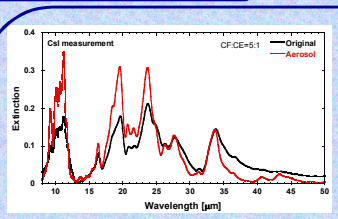

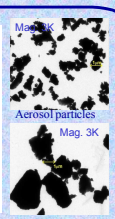

Original particles

Aerosol particles are concentrated in an impactor, and so only small-sized particles can reach the cell. We compare the spectra taken by the aerosol particles in the cell and the original sample by making use of CsI pellet technique in order to verify the size effect. The aerosol particles are captured on a ring filter when we evacuate the N_2-gas in the cell. Minor peaks are plainly appeared when the particles are small (aerosol particles), and extinction is enhanced by a factor of 2. TEM images show the particle size differences between the original and aerosol particles (Tamanai et al. submitted).

3. Morphological effect (Shape)

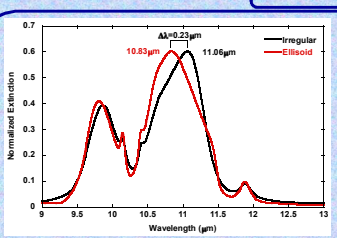

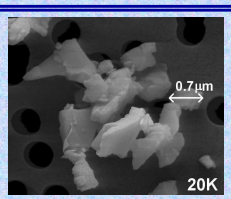

Irregular shaped particles

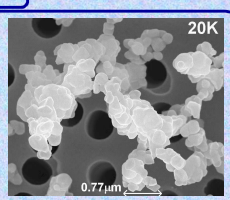

Ellipsoidal particles (roundish particles)

The spectra obtained by two types of crystalline forsterite are compared. One is the irregular shaped particles. Another is the ellipsoidal particles. The peaks of the geometrical resonances are shifted by up to 0.23μm towards shorter wavelengths for the ellipsoidal particles (Tamanai et al. 2006b).

5. Heterogeneous Dust Grains

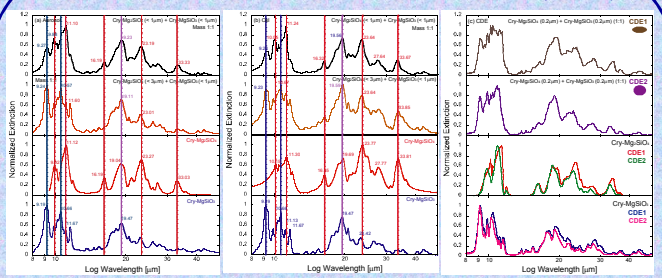

The mass proportion of *forsterite* and *enstatite* samples in the mixture is one to one. The spectra obtained by the mixed sample are influenced more by the small size particles. This trend can be seen in both aerosol and CsI pellet spectra. The spectra of mixed sample is not straightforward to interpret since all the morphological aspects exert an influence on band profiles. The theoretical calculations cannot reproduce the mixed band profiles well (Fig. (c)). (In this case, the size of the particles affects only on the strength of the extinction spectra, but not for the spectral shape itself.) In these CDE1 and CDE2 calculations, prominent peaks from one source (forsterite or enstatite) cannot be detected unlike the experimental spectra. Since the mixture contains only forsterite and enstatite, it is possible to identify the origin of each peak. The peaks of the mixed sample slightly differ from the spectral peaks measured for each individual sample (Fig. (a) & (b)). It is conceivable that relying only on the spectral peaks measured by an individual substance is insecure for the identification of observed spectra. Since observed spectra contain numerous dust grains, much more considerable variations on the band profiles are presumed to detect in the spectra. Consequently the further heterogeneous dust grain investigation is necessary to find out how much the interaction with diverse particles produces an effect on measured band profiles.

CDE (Continuous distribution of ellipsoid) (Bohren & Huffman 1983)
CDE1→ all ellipsoidal shapes with equal probability
CDE2 → most likely near-spherical shapes (Ossenkopf et al. 1992)

Acknowledgement:

We wish to thank Dr. R.T. Schmitt and Prof. Dr. D. Stöffler at Museum für Naturkunde Berlin in Humboldt-Universität zu Berlin for providing us the natural hypersthene and diopside samples. We express to the members of pathology department at FSU Jena, Dr. S. Nietzsche, F. Steiniger, and C. Kämnitz our gratitude for the technical support of TEM and SEM. We are grateful to G. Born for her assistance with sample preparations and W. Teuschel for his technical support of our experimental devices. Our project has been supported by Deutsche Forschungsgemeinschaft (DFG) under the grant MU 1164/6.

References:

Bohren, C.F., & Huffman, D.R. 1983, Absorption and Scattering of Light by Small Particles, (N.Y.: John Wiley & Sons Inc.)
Draine, B.T. 1988, ApJ, 333, 848
Mackowski, D.W., & Mishchenko, M.I. 1996, J. Opt. Soc. Am. A, 13, 2266
Mie, G. 1908 Ann. Phys., 25, 377
Min, M., Hovenier, J.W., de Koter, A., Waters, L.B.F.M., and Dominik, C., 2005, Icarus, 179, 158
Mishchenko, M.I. 1990, Ap&SS, 164, 1
Ossenkopf, V., Henning, Th., and Mathis, J.S. 1992, A&A, 261, 567
Purcell, E.M., & Pennypacker, C.R. 1973, ApJ, 186, 705
Tamanai, A., Mutschke, H., Blum, J., and Neuhäuser, R. 2006a, J. Quant. Spectrosc. Radiat, Transfer, 100, 373
Tamanai, A., Mutschke, H., Blum, J., and Meeus, G. 2006b, ApJL, 648, L147